HAL open science

Damage detection in tensegrity under varying temperature using interacting Particle-Ensemble Kalman Filter

Neha Aswal, Subhamoy Sen, Laurent Mevel

To cite this version:

Neha Aswal, Subhamoy Sen, Laurent Mevel. Damage detection in tensegrity under varying temperature using interacting Particle-Ensemble Kalman Filter. NDT-CE 2022 - International Symposium on Nondestructive Testing in Civil Engineering, Aug 2022, Zurich, Switzerland. 10.58286/27214 . hal-03874406

HAL Id: hal-03874406

https://inria.hal.science/hal-03874406v1

Submitted on 28 Nov 2022

HAL is a multi-disciplinary open access archive for the deposit and dissemination of scientific research documents, whether they are published or not. The documents may come from teaching and research institutions in France or abroad, or from public or private research centers.

L'archive ouverte pluridisciplinaire **HAL**, est destinée au dépôt et à la diffusion de documents scientifiques de niveau recherche, publiés ou non, émanant des établissements d'enseignement et de recherche français ou étrangers, des laboratoires publics ou privés.

Damage detection in tensegrity under varying temperature using interacting Particle-Ensemble Kalman Filter

Neha ASWAL[1], Subhamoy SEN[1*], Laurent MEVEL[2]

[1]Indian Institute of Technology Mandi, Mandi, India
[2]Univ. Gustave Eiffel, Inria, Cosys-SII, I4S, Campus de Beaulieu, Rennes,France
*Corresponding author, e-mail address: *subhamoy@iitmandi.ac.in*

Abstract

Tensegrities are structural mechanisms, with dedicated compression (struts/bars) and tension members (cables). The compression members float inside the network of tension members. Tensegrities are characterized by the presence of at least one infinitesimal mechanism, which is stabilized by the pre-stress present in the members, to ensure the equilibrium of the structure. Under external load, tensegrity may change its form by altering its member pre-stress, thereby affecting its global stiffness even in the absence of damage. Moreover, tensegrities can have different stiffness properties under the same structural configuration in the absence of any damage or external load, if the pre-stress levels of the members are different. However, the changes in dynamic characteristics of tensegrities are not limited to the aforementioned causes only and is also affected by ambient uncertainties. A variation in temperature may alter the dynamic characteristics of a tensegrity by influencing its material (Young's modulus, etc.) and structural (boundary conditions, structural dimensions, etc.) properties. This can potentially lead to a false impression of tensegrity damage/health.

Meanwhile, the prolonged usage of tensegrity may lead to loss of pre-stress in the cables, buckling of the bars, corrosion, and damage of the members, etc. Thus affecting the structural stiffness which leads to change in the measured dynamic properties of the tensegrity. To account for this actual damage in the tensegrity, all the mentioned major challenges that could lead to a false alarm need to be dealt with. The present study develops a vibration-based time-domain approach for tensegrity health monitoring in the presence of uncertainties due to ambient force, measurement noise, and varying temperature. An interacting filtering technique has been used, where the state variables are estimated by the Ensemble Kalman filter that resides inside the Particle filter which computes the health parameters.

Keywords: Damage detection, Bayesian filtering, Structural health monitoring, Temperature, Tensegrity.

1 Introduction

Since its introduction as an engineering structure in the 1960s [1, 2], tensegrity has found wide application in robotics (NASA superbot), aerospace (deployable telescope), civil structures (roofs, towers, bridges), biomechanics, etc. Tensegrities are defined by the presence of at least one infinitesimal mechanism which is stabilized by the prestress present in the members. They are statically indeterminate and seize to exist in the absence of member prestress. They are made of disjointed compression members (struts/bars) that float in a web of cables (tension members). While self-stiffening nature of tensegrity, i.e., change in shape to accommodate change in external load by altering prestress, makes it deployable, having dedicated compression and tension members makes it light-weight.

Further, the same characteristics that make tensegrities deployable and light-weight, necessi-

tates a highly optimised design for their construction. Tensegrities with same topology can have different stiffnesses if their pre-stress levels are not same. Moreover, they have multiple stable states (with different stiffness values) to carry various external loads. With time, cables may lose tension and bars/struts may buckle, which may lead to a catastrophic failure of this highly optimized structure. Therefore, it is necessary to regularly monitor the health of a tensegrity structure.

However very few structural health monitoring (SHM) endeavours for tensegrities have been undertaken. With struts patched with piezo transducers, [3] utilised dynamic strain measurements to assess the damage in tensegrity. Three methods to detect damage in tensegrity were compared [4], namely, frequency analysis, error-domain model falsification (EDMF) using node position measurement and moving-window principal component analysis (MWPCA) using strain measurements. Multiple stable states in tensegrity have different natural frequencies and mode shapes, which makes it difficult to attribute the change in frequencies to damage only. Results from EDMF are sensitive to the amount of ambient uncertainty. Whereas MWPCA works efficiently with high signal to noise ratio (SNR) but fails at low SNR levels.

Most of the SHM approaches for tensegrity have been defined for deterministic cases which disregard the uncertainties that prevail in SHM of real-life tensegrities. Any model-based SHM approach for a real tensegrity needs to deal with uncertainties due to unavoidable modelling error, unknown ambient forcing, and sensor (measurement) noise. Such uncertainties have been effectively dealt with Bayesian filters [5]. Bayesian filters define the structural dynamics in terms of unobserved 'states', such as, displacement, velocity, etc. by a probabilistic model called process model. The states are observed and updated with the help of probabilistic measurement model which is defined by the relationship between the states and the measurements obtained from the sensors (such as, strain, acceleration, etc.). These probabilistic models account for the uncertainties present due to model inaccuracy, external force, and measurement noise. The physical state model is converted to a discrete state-space model to compute system states. Further, health parameters are also added alongside the states to detect damage in the tensegrity. The health parameters, i.e., health indices (**HI***s*) are defined in terms of reduction in structural rigidity.

An interactive filtering technique, interacting particle ensemble Kalman filter (IPEnKF), that uses only output measurement (strain data) has been successfully utilised to detect, localize, and estimate damage in tensegrities [5]. In IPEnKF the parameters are estimated by the particle filter (PF) whereas the ensemble Kalman filter (EnKF), nested inside the PF, estimates the health parameters ($\boldsymbol{\xi}$). However, thermal variation in the surrounding environment usually masks the damage signature present in the measurement sensor output which results in false positive or negative alarms while detecting damage in the structure. Moreover, unique to tensegrities, variation in ambient temperature affects the prestress, which in turn alters their modal characteristics [6]. This may lead to ambiguous state and parameter estimation during their SHM if the associated uncertainties are not considered.

To overcome the effect of ambient temperature on SHM outcomes, a damage sensitive feature, Bayesian whiteness test was introduced [7]. Residual power spectral density (PSD) generally remains constant (approximately) for changes in dynamics properties caused due to environ-

mental variations whereas peaks are visible in the residual PSD when the changes are observed due to damage. However this method is sensitive to errors present in input process and measurement noise covariance matrices, where it is difficult to differentiate the cause (damage or error in covariance) of peaks in residual PSD. A two step approach has further been introduced where the modal parameter estimation is corrected with respect to reference temperature field (pre-processing step) and the corrected modal parameters are then utilised for damage detection [8]. However the pre-processing step is a deterministic step and further, several temperature measurements for different locations on the structure are needed which may not be feasible.

Most of the temperature-robust algorithms are defined in modal domain which associate change in modal parameter values mainly to damage and temperature condition, however modal parameters of tensegrity may change due to its shift to another stable state by alteration in its member prestress, thereby stiffness. This may result in false damage detection. Therefore, an SHM approach is proposed that can be robust to ambient temperature in detecting tensegrity health. Robustness to temperature effect is provided by incorporating the effect of ambient temperature into the state-predictor model itself through the associated material and geometric stiffnesses' relationship with the external temperature. The refined predictor model of tensegrity takes care of the ambient temperature by bringing in additional correlation between temperature and tensegrity response. Meanwhile the change in temperature from reference temperature is simultaneously estimated alongside the health parameters. Hence the algorithm is dependent only on the measurement/response sensor data.

Robustness to temperature effect is provided by incorporating the effect of ambient temperature into the state-predictor model.

2 State-space formulation incorporating thermal variation relationships

Bayesian filters transform the dynamics of the structure Before the governing differential equation (*gde*) is formulated and converted to state-space form, the effect of temperature on the tensegrity is incorporated into the *gde* itself. In the following subsections each step has been discussed individually.

2.1 Incorporation of temperature effect

The environmental thermal variation affects both material and geometric stiffnesses. In the current study, the material type of tensegrity members is assumed to be made of different grades of steel. Further temperature dependence relationship for the modulus of elasticity, E^m of each member is assumed as the following empirical relation adopted from [6, 9],

$$E^m = E^m_{20}(-0.000835T + 1.0167) \tag{1}$$

where, E^m_{20} is the modulus of elasticity of member at $20°C$ and $T = 20°C + \Delta T$.

Following linear thermal expansion formulation for the bars/struts and cables since one dimension (length) is comparatively much larger than the other two dimensions (areal), the length of element m, is given by

$$l^m = l^m_o(1 + \alpha\Delta T) \tag{2}$$

with, l_o^m being the length of element at reference temperature T_o ($= 20°C$) in present study for consistency). ΔT is the temperature increment from T_o and α is the thermal expansion coefficient.

2.2 Geometric nonlinear finite element model

Member prestress necessary for stability of tensegrity can be affected by changing environmental temperature. Moreover, tensegrity show large deformations under external load. Such type of structures are modelled by considering geometric nonlinear finite element modelling (*fem*) [5, 6, 10]. The associated strain-displacement relationship (detailed in [5]), can be exploited to arrive at the locally linearized temperature dependent time varying tangent stiffness matrix, $\mathbf{K}^m(t,T)$,

$$\mathbf{K}^m(t,T) = \frac{A^m l^m(T)}{2}\int_{-1}^{1}\frac{\partial(\mathbf{B}^{m'}\sigma^m(r,t,T))}{\partial\mathbf{q}^m(t)}dr \tag{3}$$

where, $\mathbf{B}^m$ is the sum of linear ($\mathbf{B}_L^m$) and nonlinear ($\mathbf{B}_{NL}^m$) strain-displacement matrices, $\mathbf{q}^m(t)$ is the global displacement vector, and A^m is the uniform cross section. $\mathbf{B}_{NL}^m$ is dependent on $\mathbf{q}^m(t)$, however for readability, its dependence notation has been dropped. $\sigma^m(r,t,T)$ is the second Piola-Kirchhoff stress obtained from the constitutive relation, $\sigma^m(r,t,T) = \mathbf{E}^m(t,T)\varepsilon^m(r,t)$, with $\mathbf{E}^m(t,T)$ being the constitutive matrix.

The tangential stiffness matrix ($\mathbf{K}^m(t,T)$) is further split into material ($\mathbf{K}_M^m(t,T)$), geometric ($\mathbf{K}_G^m(t,T)$), and initial displacement ($\mathbf{K}_U^m(t,T)$) stiffness matrices and is given by their summation, $\mathbf{K}^m(t,T) = \mathbf{K}_M^m(t,T) + \mathbf{K}_G^m(t,T) + \mathbf{K}_U^m(t,T)$. The stiffness matrices, $\mathbf{K}_M^m(t,T)$, $\mathbf{K}_G^m(t,T)$, and $\mathbf{K}_U^m(t,T)$, are given by the following,

$$\begin{aligned}
\mathbf{K}_M^m(t,T) &= \frac{\mathbf{E}^m(t,T)A^m l^m(T)}{2}\int_{-1}^{1}\mathbf{T}^{m'}\mathbf{B}_L^{m'}\mathbf{B}_L^m\mathbf{T}^m dr \\
\mathbf{K}_G^m(t,T) &= \frac{A^m l^m(T)}{2}\int_{-1}^{1}\frac{\partial\mathbf{B}_{NL}^{m'}}{\partial\mathbf{q}^m(t)}\sigma^m(r,t,T)\,dr \\
\mathbf{K}_U^m(t,T) &= \frac{\mathbf{E}^m(t,T)A^m l^m(T)}{2}\int_{-1}^{1}\mathbf{T}^{m'}(\mathbf{B}_L^{m'}\mathbf{B}_{NL}^m + \mathbf{B}_{NL}^{m'}\mathbf{B}_L^m + \mathbf{B}_{NL}^{m'}\mathbf{B}_{NL}^m)\mathbf{T}^m dr
\end{aligned} \tag{4}$$

with $\mathbf{T}^m$ being the member-specific transformation matrix. The dependency of stiffness matrices on temperature (T) is because of the thermal expansion effect on structural configuration (through $l^m(T)$) and temperature-dependence of $E^m(T)$.

2.3 State-space formulation

The *gde* for tensegrity is defined as,

$$\mathbf{M}\ddot{\mathbf{q}}(t) + \mathbf{C}(t,T)\dot{\mathbf{q}}(t) + \mathbf{P}(\mathbf{q}(t),T) = \mathbf{F}(t) \tag{5}$$

with $\mathbf{M}$ being the time and temperature invariant global mass matrix, and $\mathbf{P}(\mathbf{q}(t),T)$ being the time variant inelastic resisting force. $\mathbf{P}(\mathbf{q}(t),T)$, is nonlinear as geometric nonlinearity is considered in the *fe* model of tensegrity. $\mathbf{C}(t,T)$ is the Rayleigh damping which is dependent on mass and resisting force, making it dependent on $\mathbf{q}^m(t)$, hence nonlinear [5]. The time

dependency in $\mathbf{P}(\mathbf{q}(t), T)$ is also due to the varying health condition of the tensegrity apart from varying stable states. External ambient force, $\mathbf{F}(t)$ is modeled as zero mean white Gaussian noise (WGN). $\mathbf{q}(t), \dot{\mathbf{q}}(t)$ and $\ddot{\mathbf{q}}(t)$ are $n \times 1$ order displacement, velocity, and acceleration response at the nodes.

The discrete form of Equation (5) is given by,

$$\mathbf{M}\Delta\ddot{\mathbf{q}}_k + \mathbf{C}_k\Delta\dot{\mathbf{q}}_k + \mathbf{K}_k\Delta\mathbf{q}_k = \Delta\mathbf{F}_k \tag{6}$$

where, operator Δ denotes the corresponding increment over each time step.

The nonlinear state transition function for tensegrity is defined in discrete time state-space formulation as,

$$\mathbf{x}_k = f(\mathbf{x}_{k-1}, \mathbf{M}, \mathbf{K}_k, \mathbf{C}_k, dt, T, \mathbf{v}_k) \ , \text{ where } \mathbf{v}_k \sim \mathcal{N}(0, \mathbf{Q}) \tag{7}$$

here, $\mathbf{x}_k = [\mathbf{q}_k \ \dot{\mathbf{q}}_k \ \ddot{\mathbf{q}}_k]'$, i.e., the discrete definition of the system states (displacement, velocity, and acceleration) evolving over the nonlinear state propagation function $f(\bullet)$. $\mathbf{M}$, $\mathbf{K}_k$, and $\mathbf{C}_k$ are the discrete mass, stiffness, and damping matrices. dt is the time step for discretization. $\mathbf{v}_k$ is the process noise. Subsequently, the measurement equation can be defined as,

$$\varepsilon_k = \mathbf{HB}(\mathbf{x}_k) + \mathbf{w}_k \ , \text{ where } \mathbf{w}_k \sim \mathcal{N}(0, \mathbf{R}) \tag{8}$$

where, $\mathbf{B}(\bullet)$ denotes the global nonlinear strain-displacement relationship for all members with $\mathbf{x}_k$ being its argument. ε_k consists of all the recorded member strains. $\mathbf{H}$ is the selection matrix that isolates the measured member strains from all the predicted set. $\mathbf{w}_k$ is the measurement noise.

For system simulation, explicit Newmark-beta method has been employed which can explicitly solve the incremental equilibrium equation (cf. Equation (6)) with acceptable accuracy [11].

3 Interacting particle ensemble Kalman filter

The states and parameters are estimated using previously developed IPEnKF algorithm [5]. The error in measurement prediction when compared to actual output obtained from sensors, is attributed to change in material stiffness, due to damage and temperature. Damage is replicated by a reduction in initial modulus of elasticity, E_0^m, using health indices ($\boldsymbol{\xi}_k$) as $S_k(\boldsymbol{\xi}_k) = S_0 \cdot \boldsymbol{\xi}_k$. Here S_0 is the vector encompassing the initial axial stiffness of all the tensegrity members ($S_0 = \left[\left(E_0^1 A_0^1\right), \left(E_0^2 A_0^2\right), \ldots \left(E_0^m A_0^m\right)\right]$). Meanwhile the effect of temperature is observed by estimating ΔT alongside $\boldsymbol{\xi}_k$. Following the temperature and $E^m(T)$ relation (from [9]), temperature effect is neutralized for S_k. Therefore, $\boldsymbol{\xi}_k$ traces the alteration in the material stiffness of all the members of tensegrity, thereby detecting damage.

Following [5], PF estimates the parameters while EnKF nestled inside the PF, estimates the state variables. Initial particle evolution in time is considered as a Gaussian perturbation around the current estimate of the particle, $\xi_k^j = \beta\xi_{k-1}^j + \mathcal{N}\left(\delta\xi_k; \sigma_k^\xi\right)$. β is a hyper-parameter that controls the turbulence in the estimation. The particles are then put through the nested EnKF for state estimation. Within EnKF, N_e state ensembles are propagated through the system (cf. Equation (7)). For this, current estimate for the stiffness matrix $\mathbf{K}_k$ is obtained and prior state

ensembles are propagated to the next time step, $\mathbf{x}^{i,j}_{k|k-1}$. Subsequently, the propagated ensembles are observed through measurement predictions, $\varepsilon^{i,j}_{k|k-1}$. The process and measurement equations for the system are presented in the following,

$$\begin{aligned}
\mathbf{x}^{i,j}_{k|k-1} &= f\left(\mathbf{x}^{i,j}_{k-1|k-1}, \mathbf{M}, \mathbf{K}^{i,j}_{k|k-1}(\xi^j_{k-1}), \mathbf{C}^{i,j}_{k|k-1}, dt, T^j_{k-1}, \mathbf{v}^{i,j}_k\right), \text{ where } \mathbf{v}^{i,j}_k \sim \mathscr{N}(0, \mathbf{Q}) \\
\varepsilon^{i,j}_{k|k-1} &= \mathbf{HB}(\mathbf{x}^{i,j}_{k|k-1}) + \mathbf{w}^{i,j}_k, \text{ where } \mathbf{w}^{i,j}_k \sim \mathscr{N}(0, \mathbf{R})
\end{aligned} \tag{9}$$

Next, the predicted measurement, $\varepsilon^{i,j}_{k|k-1}$, is compared with the actual measurement and innovation, $I^{i,j}_k$, is obtained. Further, ensemble mean of innovation, ε^j_k, propagated state estimates, $\mathbf{x}^j_{k|k-1}$, and predicted measurements, $\varepsilon^j_{k|k-1}$, are obtained with the measurement prediction covariance, $C^{j,yy}_k$ and cross-covariance, $C^{j,xy}_k$ [5].

The innovation error covariance, $\mathbf{S}^j_k$, and EnKF gain, $\mathbf{G}^j_k$, are then obtained as $\mathbf{S}^j_k = C^{j,yy}_k + \mathbf{R}$ and $\mathbf{G}^j_k = C^{j,xy}_k \left(\mathbf{S}^j_k\right)^{-1}$. With this gain, the state ensembles are updated as,

$$\mathbf{x}^{i,j}_{k|k} = \mathbf{x}^{i,j}_{k|k-1} + \mathbf{G}^j_k \varepsilon^{i,j}_k \tag{10}$$

Finally, likelihood of each particle is calculated as, $\mathscr{L}\left(\xi^j_k\right) = \frac{1}{(2\pi)^n \sqrt{\left|\mathbf{S}^j_k\right|}} e^{-0.5\varepsilon^{j'}_k \mathbf{S}^{j^{-1}}_k \varepsilon^j_k}$. The normalized weight for each jth particle is further obtained using corresponding likelihood, $w\left(\xi^j_k\right) = \frac{w\left(\xi^j_{k-1}\right)\mathscr{L}\left(\xi^j_k\right)}{\sum_{j=1}^N w\left(\xi^j_{k-1}\right)\mathscr{L}\left(\xi^j_k\right)}$. The particle approximations for the states and parameters are then estimated as their weighted mean, given by the following,

$$\mathbf{x}_{k|k} = \sum_{j=1}^{N} w(\xi^j_k)\mathbf{x}^j_{k|k}; \quad \text{and} \quad \boldsymbol{\xi}_{k|k} = \sum_{j=1}^{N} w(\xi^j_k)\xi^j_k \tag{11}$$

3.1 Proposed methodology for robustness against temperature

The initial SHM algorithm [5] for tensegrity has been improved for robustness against the effect of temperature on damage detection. Steps pertaining to the SHM of tensegrity robust to temperature effects has been provided in the following,

Proposed thermal variation-robust IPEnKF algorithm

Step 1. Define a reference temperature and the initial geometrical and material properties of tensegrity (see Section 2.1).

Step 2. Initialize parameters (particles), $\xi^j_0 = [\boldsymbol{\xi} \;\; \Delta T]^j_0$, state estimates (ensembles), $X^{i,j}_{0|0}$, and state error covariance $P^{i,j}_{0|0}$.

Particle filter

Step 3. Evolve parameters for each jth particle to current time step ($k-1$ to k).

Ensemble Kalman filter

Step 4. Define external force as a white Gaussian noise.

Step 5. Obtain stiffness matrix for current time-step and define system matrices (see Section 2.2).

Step 6. Predict states, $X^{i,j}_{k|k-1}$ and measurement $\varepsilon^{i,j}_{k|k-1}$ for each ith ensemble (See Equation (9)).

Step 7. Calculate innovation, i.e., departure of predicted from actual measurement; cross-covariance between the state and the measurement prediction; and the innovation covariance.

Step 8. Compute EnKF gain and correct the predicted states (see Equation (10)).

end Ensemble Kalman filter

Step 9. Calculate likelihood and weight for each particle and resample particles accordingly.

end Particle filter

Step 10. Update the states and parameters as their weighted mean (see Equation (11)).

Repeat from Step 2. till the last time iteration is reached.

4 Numerical Results

The proposed algorithm has been numerically tested on a simplex tensegrity. A simplex is a cylindrical tensegrity with 3 bars and 6 cables (cf. Figure 1). The initial statically stable coordinates have been taken from [5]. The coordinates and the connectivity of members for simplex has been given in Table 1. All the members, cables and bars, are assumed to be made of steel with $E^m_{20} = 200\ GPa$. The diameters of bar and cable members are taken as 20 mm and 5 mm, respectively. For dynamic analysis, the simplex is connected to a fixed base at three nodes (1-3). The stable simplex is further excited with an ambient Gaussian force applied on the fourth node, in x-direction.

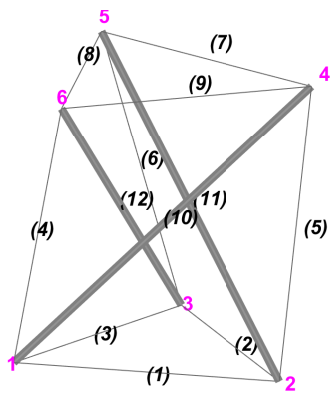

Figure 1: Simplex tensegrity configuration

Table 1: Nodal coordinates, elemental connectivity and initial tension coefficients of simplex tensegrity (*with c:cable and b:bar*)

	Node	1	2	3	4	5	6
ST	X	0.577	-0.244	-0.266	-0.452	0.0094	0.509
	Y	0	0.5	-0.461	0.301	-0.542	0.279
	Z	0	0	0	0.919	0.919	0.919

	Element	1	2	3	4	5	6	7	8	9	10	11	12
ST	Node 1	1	2	3	1	2	3	4	5	6	1	2	3
	Node 2	2	3	1	6	4	5	5	6	4	4	5	6
	Type	*c*	*c*	*c*	*c*	*c*	*c*	*c*	*c*	*c*	*b*	*b*	*b*
	Initial tension coeff. (N/m)	0.6834			1.1837			0.6835			-1.1838		

The initial distribution type for the parameter particles, $\boldsymbol{\xi}_k$ (**HI**s) is set to be Gaussian, with a mean of 1 (undamaged condition) and a standard deviation of 0.02. β is selected to be 0.90 (cf. Section 3). 1500 particles with 50 ensembles have been chosen for IPEnKF. A reference temperature of $20°C$ has been considered. Sampling frequency of 100 Hz has been utilised in the simulation. The simulation is done at an ambient temperature of $40°C$ for a total of 5 s. A 40% damage is introduced in the eleventh member 0.5s after the start of simulation. From Figure 2 it is clear that the original IPEnKF (which is not robust to temperature variation) is inefficient in correct estimation of health indices. Hence, the current temperature - robust IPEnKF algorithm has been introduced.

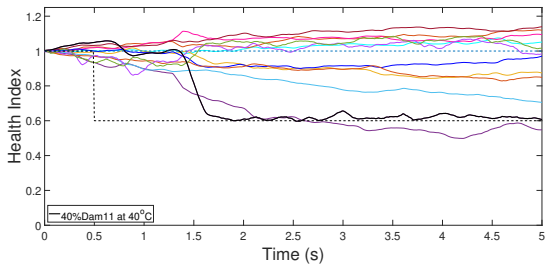

Figure 2: Damage detection by the original IPEnKF [5] (ambient temperature = $40°C$).

The same simulated measurement output that was provided to the original IPEnKF, is fed to the proposed temperature - robust algorithm. The ambient temperature and health parameters are estimated simultaneously. The initial distribution type for the parameter particles corresponding to ΔT ($\in \xi_0^j$), is set to be Gaussian, with a mean of 5 and a standard deviation of 2.5, with the rest of IPEnKF details remaining the same as mentioned before. Figure 3a depicts the capability of the proposed algorithm to estimate ambient temperature in real-time. Initialized at $20°C$, the ambient temperature approximated near the actual temperature provided in the simulation, i.e., $40°C$. More importantly, the algorithm has accurately detected correct damage level for the eleventh member without any false alarms, with an **HI** $= 0.6$ corresponding to the inflicted damage level of 40% (cf. Figure 3b). Thus, suggesting that the temperature effect has been neutralized.

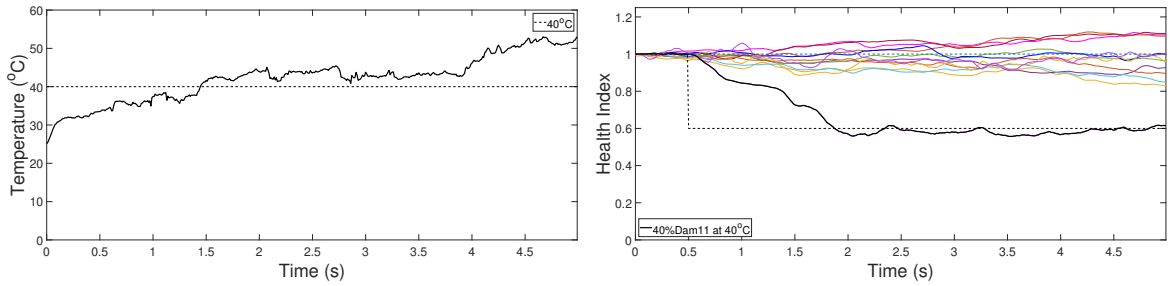

(a) Estimated ambient temperature **(b)** Damage detection (ambient temperature = 40°C)

Figure 3: Estimation of ambient temperature and health indices by proposed temperature-robust IPEnKF algorithm (ambient temperature = 40°C).

5 Conclusion

Thermal variation usually masks the effect of structural damage on the measurement response which may lead to misleading results. A novel temperature-robust health monitoring approach has been developed for tensegrities that achieved robustness against the effect of thermal variation on damage signature by incorporating the effect of temperature in to the state-predictor model. Interacting filtering technique (IPEnKF) is further utilized to simultaneously detect damage as well as the ambient temperature. Thus the estimated ambient temperature is utilised for the state-predictor model rendering the need of regularly measuring temperature at various points of the structure. The proposed algorithm accurately detects damage in the structure without any false positives. It is capable of separating the effect of temperature and damage on the response, targeting temperature robust damage detection in tensegrities.

Acknowledgement

This study was funded by Science & Engineering Research Board (SERB), New Delhi, India, through grant file no. ECR/2018/001464.

References

[1] K. Snelson, *Tensegrity Masts*. 1973.

[2] F. R. Buckminster, "Tensile-integrity structures," Nov. 13 1962. US Patent 3,063,521.

[3] S. Bhalla, R. Panigrahi, and A. Gupta, "Damage assessment of tensegrity structures using piezo transducers," *Meccanica*, vol. 48, no. 6, pp. 1465–1478, 2013.

[4] A. C. Sychterz and I. F. Smith, "Using dynamic measurements to detect and locate ruptured cables on a tensegrity structure," *Engineering Structures*, vol. 173, pp. 631–642, 2018.

[5] N. Aswal, S. Sen, and L. Mevel, "Estimation of local failure in tensegrity using Interacting Particle-Ensemble Kalman Filter," *Mechanical Systems and Signal Processing*, vol. 160, p. 107824, 2021.

[6] N. Ashwear and A. Eriksson, "Influence of temperature on the vibration properties of tensegrity structures," *International Journal of Mechanical Sciences*, vol. 99, pp. 237–250, 2015.

[7] K. Erazo, D. Sen, S. Nagarajaiah, and L. Sun, "Vibration-based structural health monitoring under changing environmental conditions using Kalman filtering," *Mechanical systems and signal processing*, vol. 117, pp. 1–15, 2019.

[8] M. D. H. Bhuyan, G. Gautier, N. Le Touz, M. Döhler, F. Hille, J. Dumoulin, and L. Mevel, "Vibration-based damage localization with load vectors under temperature changes," *Structural Control and Health Monitoring*, vol. 26, no. 11, p. e2439, 2019.

[9] N. D. Kankanamge and M. Mahendran, "Mechanical properties of cold-formed steels at elevated temperatures," *Thin-Walled Structures*, vol. 49, no. 1, pp. 26–44, 2011.

[10] K. Kebiche, M. Kazi-Aoual, and R. Motro, "Geometrical non-linear analysis of tensegrity systems," *Engineering structures*, vol. 21, no. 9, pp. 864–876, 1999.

[11] P. Pan, T. Wang, and M. Nakashima, *Development of online hybrid testing: Theory and applications to structural engineering*. Butterworth-Heinemann, 2015.